Dear Author,

Here are the proofs of your article.

- You can submit your corrections **online**, via **e-mail** or by **fax**.
- For **online** submission please insert your corrections in the online correction form. Always indicate the line number to which the correction refers.
- You can also insert your corrections in the proof PDF and **email** the annotated PDF.
- For fax submission, please ensure that your corrections are clearly legible. Use a fine black pen and write the correction in the margin, not too close to the edge of the page.
- Remember to note the **journal title**, **article number**, and **your name** when sending your response via e-mail or fax.
- **Check** the metadata sheet to make sure that the header information, especially author names and the corresponding affiliations are correctly shown.
- **Check** the questions that may have arisen during copy editing and insert your answers/ corrections.
- **Check** that the text is complete and that all figures, tables and their legends are included. Also check the accuracy of special characters, equations, and electronic supplementary material if applicable. If necessary refer to the *Edited manuscript*.
- The publication of inaccurate data such as dosages and units can have serious consequences. Please take particular care that all such details are correct.
- Please **do not** make changes that involve only matters of style. We have generally introduced forms that follow the journal's style.
  Substantial changes in content, e.g., new results, corrected values, title and authorship are not allowed without the approval of the responsible editor. In such a case, please contact the Editorial Office and return his/her consent together with the proof.
- If we do not receive your corrections **within 48 hours**, we will send you a reminder.
- Your article will be published **Online First** approximately one week after receipt of your corrected proofs. This is the **official first publication** citable with the DOI. **Further changes are, therefore, not possible.**
- The **printed version** will follow in a forthcoming issue.

Please note

After online publication, subscribers (personal/institutional) to this journal will have access to the complete article via the DOI using the URL: http://dx.doi.org/[DOI].
If you would like to know when your article has been published online, take advantage of our free alert service. For registration and further information go to: http://www.link.springer.com.

Due to the electronic nature of the procedure, the manuscript and the original figures will only be returned to you on special request. When you return your corrections, please inform us if you would like to have these documents returned.

Metadata of the article that will be visualized in OnlineFirst

ArticleTitle	Heterogeneous Photocatalytic Degradation of Ibuprofen Over TiO_2–Ag Supported on Activated Carbon from Waste Tire Rubber	
Article Sub-Title		
Article CopyRight	Springer Science+Business Media, LLC, part of Springer Nature (This will be the copyright line in the final PDF)	
Journal Name	Topics in Catalysis	
Corresponding Author	Family Name	**Suarez-Escobar**
	Particle	
	Given Name	**A. F.**
	Suffix	
	Division	GIPSI Group/Department of Chemical Engineering
	Organization	Universidad de Bogotá Jorge Tadeo Lozano
	Address	Street 4 # 22-61, 110311, Bogota, Colombia
	Phone	
	Fax	
	Email	andresf.suareze@utadeo.edu.co
	URL	
	ORCID	http://orcid.org/0000-0002-7459-6041
Author	Family Name	**Conde-Rivera**
	Particle	
	Given Name	**L. R.**
	Suffix	
	Division	GIPSI Group/Department of Chemical Engineering
	Organization	Universidad de Bogotá Jorge Tadeo Lozano
	Address	Street 4 # 22-61, 110311, Bogota, Colombia
	Phone	
	Fax	
	Email	
	URL	
	ORCID	http://orcid.org/0000-0002-4408-3667
Author	Family Name	**Lopez-Suarez**
	Particle	
	Given Name	**F. E.**
	Suffix	
	Division	GIPSI Group/Department of Chemical Engineering
	Organization	Universidad de Bogotá Jorge Tadeo Lozano
	Address	Street 4 # 22-61, 110311, Bogota, Colombia
	Phone	
	Fax	
	Email	

	URL	
	ORCID	http://orcid.org/0000-0003-4129-1329
Author	Family Name	**Illán-Gómez**
	Particle	
	Given Name	**M. J.**
	Suffix	
	Division	Department of Inorganic Chemistry
	Organization	University of Alicante
	Address	Ap. 99 San Vicente del Raspeig, 03080, Alicante, Spain
	Phone	
	Fax	
	Email	
	URL	
	ORCID	http://orcid.org/0000-0002-5017-5891
Author	Family Name	**Gonzalez-Hernandez**
	Particle	
	Given Name	**K. S.**
	Suffix	
	Division	GIPSI Group/Department of Chemical Engineering
	Organization	Universidad de Bogotá Jorge Tadeo Lozano
	Address	Street 4 # 22-61, 110311, Bogota, Colombia
	Phone	
	Fax	
	Email	
	URL	
	ORCID	http://orcid.org/0000-0001-7290-7638
Author	Family Name	**Chalapud-Morales**
	Particle	
	Given Name	**J. S.**
	Suffix	
	Division	GIPSI Group/Department of Chemical Engineering
	Organization	Universidad de Bogotá Jorge Tadeo Lozano
	Address	Street 4 # 22-61, 110311, Bogota, Colombia
	Phone	
	Fax	
	Email	
	URL	
	ORCID	http://orcid.org/0000-0003-2606-0952

Schedule	Received	
	Revised	
	Accepted	

Abstract

In recent years it has been discovered that some common use medicines, such as ibuprofen and other nonsteroidal anti-inflammatory drugs, are found in water sources in concentrations that have the potential to affect aquatic organisms. On the other hand, waste used tires are a massive problem for the environment due to the leaching of toxic compounds to soils and water. Also, the exposition to environmental

	conditions can make them sources of vectors like mosquitoes. In this work, three activated carbon (AC) catalysts derived from waste tire rubber, titanium dioxide and silver were synthesized using the sol–gel method. Morphological characterizations such as SEM and TEM were performed in which, the agglomeration of titanium particles and silver crystals on the surface of the AC is evident. In the XRD analysis, the presence of elemental silver nanoparticles was detected. In the diffuse reflectance spectroscopy analysis, the decrease in the titanium band gap, as well as activity in the visible spectrum, was observed. The photocatalytic tests were performed at pH 3 and 7 in the presence of UV/Vis radiation. These tests show that there are differences between the catalyst in both, UV and visible regions. Adsorption is a major phenomenon for the removal of ibuprofen, followed by photolytic decomposition. In visible spectra, the catalysts show a good performance for the removal of ibuprofen.
Keywords (separated by '-')	Photocatalysis - Ibuprofen - Tire rubber - Emerging contaminant - Activated carbon
Footnote Information	

Topics in Catalysis
https://doi.org/10.1007/s11244-020-01311-1

ORIGINAL PAPER

Heterogeneous Photocatalytic Degradation of Ibuprofen Over TiO_2–Ag Supported on Activated Carbon from Waste Tire Rubber

A. F. Suarez-Escobar[1] · L. R. Conde-Rivera[1] · F. E. Lopez-Suarez[1] · M. J. Illán-Gómez[2] · K. S. Gonzalez-Hernandez[1] · J. S. Chalapud-Morales[1]

Abstract

In recent years it has been discovered that some common use medicines, such as ibuprofen and other nonsteroidal anti-inflammatory drugs, are found in water sources in concentrations that have the potential to affect aquatic organisms. On the other hand, waste used tires are a massive problem for the environment due to the leaching of toxic compounds to soils and water. Also, the exposition to environmental conditions can make them sources of vectors like mosquitoes. In this work, three activated carbon (AC) catalysts derived from waste tire rubber, titanium dioxide and silver were synthesized using the sol–gel method. Morphological characterizations such as SEM and TEM were performed in which, the agglomeration of titanium particles and silver crystals on the surface of the AC is evident. In the XRD analysis, the presence of elemental silver nanoparticles was detected. In the diffuse reflectance spectroscopy analysis, the decrease in the titanium band gap, as well as activity in the visible spectrum, was observed. The photocatalytic tests were performed at pH 3 and 7 in the presence of UV/Vis radiation. These tests show that there are differences between the catalyst in both, UV and visible regions. Adsorption is a major phenomenon for the removal of ibuprofen, followed by photolytic decomposition. In visible spectra, the catalysts show a good performance for the removal of ibuprofen.

Keywords Photocatalysis · Ibuprofen · Tire rubber · Emerging contaminant · Activated carbon

1 Introduction

The human being has created different chemical products to improve their life quality. Among these are personal care products, detergents, pesticides, medicines, among others, commonly known as emerging pollutants. The intensive use of these products generates a great problem for the environment, because there is a continuous discharge of compounds that nature by itself can not process. Also, the conventional water treatment systems are not prepared for the removal of those substances. Even though there is legislation for the discharges of agrochemicals, is not usual that the countries have regulation related to the discharge of pharmaceutical and household products, hence their release is not regulated [1, 2].

The main problem of emerging pollutants lies in the fact that their concentration is continually increasing, and so is the potential ecological impact. Also, the ecotoxicity of many of them is unknown. As an additional concern, some of them might be harmless, but its degradation products could be toxic [3, 4].

(RS)-2-(4-(2-methylpropyl)phenyl)propanoic acid, commonly known as ibuprofen, is an NSAID, commonly used as an analgesic and antipyretic. Ibuprofen is one of the 10 drugs with the highest sales worldwide, due to its efficiency as an analgesic, since its structure imitates arachidonic acid, which causes the inhibition of the cyclooxygenase-1 and cyclooxygenase-2 enzymes, avoiding the formation of prostaglandins that are responsible for inflammation and contribute to the perception of pain. The therapeutic dose of this compound ranges from 200 to 1200 mg day [2], its half-life depends on the environment in which it is found, remaining between 31 and 41 days in soils [5–7] while in water it is in the range of 60 to 100 days [8].

✉ A. F. Suarez-Escobar
andresf.suareze@utadeo.edu.co

[1] GIPSI Group/Department of Chemical Engineering, Universidad de Bogotá Jorge Tadeo Lozano, Street 4 # 22-61, 110311 Bogota, Colombia

[2] Department of Inorganic Chemistry, University of Alicante, Ap. 99 San Vicente del Raspeig, 03080 Alicante, Spain

From sales data of ibuprofen in the United States since 1990, it is estimated that more than 3000 tons have been consumed. European countries such as Germany reported in 2001 that consumption was 350 tons, while in Spain it was 276 tons for 2003, in Asian countries such as Japan, per capita consumption of ibuprofen was estimated at 0.78 g/person/year [2].

The pharmaceutical compounds have a lipophilic character (high-fat solubility, low solubility in polar compounds) that during the biotransformation process have two phases. In the first one, the hydrolysis and reduction of these compounds occurs, modifying the original molecule, while in the second phase, endogenous groups are added, which increase the polarity in the molecule. Both, the original molecules that failed to transform and the metabolites of the biotransformation are excreted by the kidneys. Approximately 15% of ibuprofen is excreted unchanged, while the other part is excreted in the form of metabolites such as hydroxy-ibuprofen, carboxy-ibuprofen, among others [2].

Medications such as ibuprofen are designed to penetrate membranes, receptors, enzymes to perform a therapeutic action on a target organism, however, it can have adverse effects on other organisms, especially in frogs and fish. The lowest concentration at which adverse effects have been reported is 0.01 µg/L [2].

There are several methods to carry out the degradation of ibuprofen, some of them involve biological treatments or membrane bioreactors. Different studies of the use of activated carbons (AC) for the removal of ibuprofen have been reported in the literature. In [9], two commercial AC, different charges of ibuprofen, and pH were used. It was shown that pH 7 gave better results, giving efficiencies of 99.8% for an initial concentration of 200 ppm. In [10], two carbons were prepared, starting from coffee waste as a precursor, one under chemical activation, and the other with additional treatment with steam. The coal with the two treatments presented efficiencies of up to 100%. In [11], degradation was performed at pH between 6 and 10, obtaining a removal at 64% and 60% respectively.

In recent years, the so-called Advanced Oxidation Processes (AOPs) have been studied in-depth, which consist of the oxidation in an aqueous medium to generate highly reactive species such as the hydroxyl radical (·OH). It is characterized by being a non-selective oxidizing agent that attacks organic molecules through dehydrogenation and/or hydroxylation reactions, allowing better mineralization of the contaminant while generating carbon dioxide, water, and some inorganic compounds [2, 12].

AOPs can be divided into two large groups; homogeneous and heterogeneous. The first one may or may not require the input of energy. Some of these methods are Fenton, modified Fenton reactions, sonolysis, among others. In the case of drug removal, heterogeneous photocatalysis based on semiconductors, ozonation, and Fenton is use [2, 3].

Different semiconductors and combinations of these are used in heterogeneous photocatalysis process to remove and degrade organic compounds from aqueous solutions [13]. Some of the semiconductors commonly evaluated are TiO_2, CdS, ZnS, Fe_2O_3, Ag/TiO_2 [14]. The TiO_2 is the most widely used semiconductor due to its high efficiency, low cost, low toxicity, and its thermal and electrical properties [14, 15]. Looking to improve the properties of this semiconductor, certain modifications are usually made to reduce the prohibited band, which is the energy difference between the valence and conduction bands; the energy that must be exceeded to carry out the photocatalytic process. An alternative to lower this barrier is to dope or couple the TiO_2 with some transition metal like Au, Pt, Cr, Ag among others. The photocatalytic activity can also be improved by the addition of non-metallic elements such as carbon, nitrogen, sulfur, chlorine, and others. The improvement in activity can be correlated to the amount of these elements [16].

In the case of silver doping, the benefits of adding silver have been demonstrated since in semiconductors it has been found that the combination of the substrate, semiconductor and metals, improves the photocatalytic process [16]. Among the options that involve the addition of nonmetals is the support of semiconductors on AC. The large surface area allows it to adsorb different compounds, having a preference for slightly polar and non-ionic molecules [17, 18], inhibits the recombination of the electron–hole pair, also, provides a surface that favors photocatalytic activity [15]. When using titanium dioxide there is an additional factor that influences the photocatalytic process and that is the phase in which the Titanium is found. Titanium has three phases, anatase, rutile, and brookite, each with different crystalline structures and prohibited bands. The rutile band gap is known to be 3.0 eV, while the anatase band gap is 3.2 eV [19] this would imply that the rutile phase as it has a smaller band will be better for the photocatalytic process, however, it has been shown anatase trends to be more active because it has a larger crystal size [20].

The photocatalytic reaction in a semiconductor like TiO_2 occurs when a photon with energy equal to or greater than that of the prohibited band excites an electron (e−), from the valence band to the conduction band, generating a hole in the valence band (h+), as shown in Fig. 1a. The generated carrier charges can recombine and migrate to the surface where they can react with electron acceptors or donors. The hole that is generated acts as an oxidizing agent that can react with a pollutant, or with water to generate hydroxyl radicals that oxidize the substance, while the electron in the conduction band acts as a reducing agent, with the oxygen producing radical superoxides. This series of reactions prevent the recombination of the electron–hole pair, which

Journal : Large 11244 | Article No : 1311 | Pages : 14 | MS Code : 1311 | Dispatch : 4-7-2020

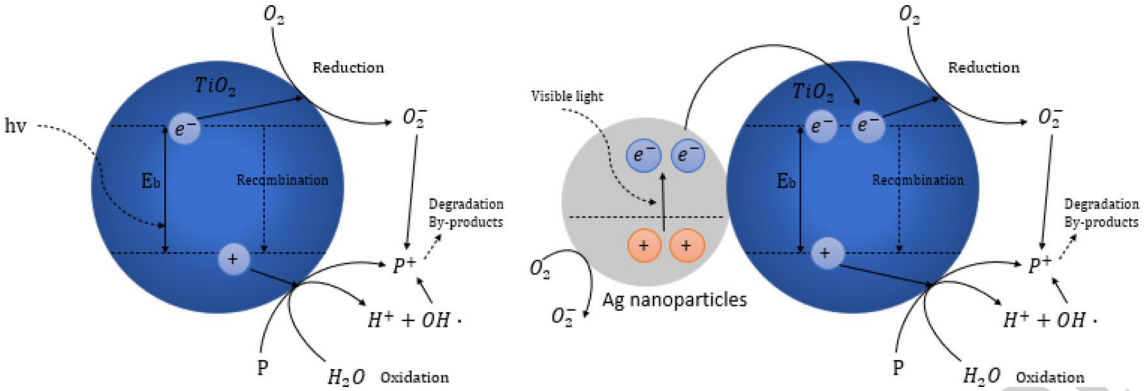

Fig. 1 Description of the photocatalytic process **a** unmodified and **b** silver modified

increases photooxidation and the efficiency of the process [2, 15, 21]. It should be noted that due to the prohibited band of TiO_2, these reactions occur with UV radiation. When doping with silver nanoparticles, these become photoexcited due to plasmon resonance, which causes the photoexcited electrons to migrate to the TiO_2 conduction band at a lower bandgap, as illustrated in Fig. 1b, also the high crystallinity of silver decreases the electron–hole pair recombination [22, 23].

There are various methods for the preparation of AC/TiO_2 (these combinations are often called as integrated photocatalytic adsorbents or by their acronym in English IPCA), which can be divided into wet and dry. The first ones consist of using a physical and/or gaseous process, such as chemical vapor deposition, while, in wet methods, an aqueous phase is used to impregnate titanium dioxide. Examples of these methods are sol–gel, impregnation, liquid phase deposition, or electrophoretic deposition [24].

In the sol–gel method, the catalyst TiO_2 is prepared from a Ti precursor such as tetrabutyl orthotitanate which is dissolved in absolute ethanol. The addition of a base or an acid is made to promote the condensation reaction or hydrolysis of the alkoxide [25]. AC can be added in different ways, such as: placing the coating of the solution on the carbon, stirring and immersing the carbon in the solution or ultrasound of the TiO_2 slurry with coal. After this, low-temperature heat treatments are carried out in the air, and later calcination at 300–800 °C in an inert atmosphere [24]. The sol–gel process is used to support TiO_2 on a matrix such as silica, AC, among others, to avoid coagulation, since it has been shown that TiO_2 tends to coagulate during the photocatalytic process, which is not convenient since it hinders the incidence of light.

Carbon can be used to support TiO_2. AC can be obtained from a large number of precursors, which are characterized by high carbon and low ash content and, where possible, low cost. In this sense, the rubber of used tires has gained interest, since used tires are an abundant waste that generates a series of environmental and health problems due to their bad disposal, generating contamination of water, soil and air [26]. Tires can store water, which is ideal for the growth of vectors such as mosquitoes, among other pests [27]. Also, it can generate toxic leachates to aquatic organisms [28]. Burning used tires generates different toxic emissions with compounds containing sulfur or benzene, as well as particulate material [29].

Given the high carbon content, the waste tires are ideal to obtain AC to be used as an adsorbent for the elimination of toxic elements such as [30, 31] phenols, pesticides, and dyes, among other molecules [32].

Taking all of the above into account, in this work a TiO_2 catalyst was synthesized, supported on AC from waste tires and dopped with silver (Ag) particles, to favor its photocatalytic performance in the degradation of ibuprofen in an aqueous medium in the UV/Vis spectrum. The results of this work could favor the generation of alternatives to mitigate two environmental problems, namely the waste tires in the environment, and the effective degradation of ibuprofen using solar radiation.

2 Experimental

2.1 Reactants

Titanium(IV) isopropoxide (Alpha Aesar, 95%) was used as a titanium precursor. 2-Propanol (JT Baker). Hydrochloric acid (Merk, 37% m/m, 2 N). Sodium hydroxide (Merk, 2 N). TiO_2 P25 9 (Degussa), Silver nitrate (Biopharchem, 99.9%). AC was prepared from tire rubber that was supplied by a local recycling company. Acetone (Merk).Comercial ibuprofen 99% was supplied by a local pharmaceutical company.

2.2 Preparation of Activated Carbon from Waste Tire Rubber

The waste tire rubber was subjected to a grinding process in a disk mill and sieving, with standard 5 and 40 mesh sieves, to obtain a particle size between 0.425 and 4 mm. Metallic

Journal : Large 11244 | Article No : 1311 | Pages : 14 | MS Code : 1311 | Dispatch : 4-7-2020

particles were removed from the material using a magnet, the residue was washed with distilled water until clear filtering water was obtained, and then, the material was dried at 80 °C for 24 h.

Finally, the sample was calcined in a nitrogen atmosphere at 400 °C for 1 h and was physically activated with CO_2 (400.0 mL/min) at 900 °C for 3 h in a fixed-bed reactor, equipped with a K-type thermocouple and a temperature controller (± 1 °C).

2.3 Determination of Specific Surface Area of Activated Carbon

The specific surface area of AC was determined with the BET method (Brunauer–Emmett–Teller) from Nitrogen adsorption isotherm at 77 K according to ASTM D6556—17 standard, in a Gemini VII 2390 Surface Area Analyzer.

2.4 Proximate Analysis of Activated Carbon

Proximate analysis (moisture, ash, volatile matter and fixed carbon) of AC was carried out following ASTM D3172 standard.

2.5 Synthesis of Catalysts

The synthesis of the catalysts was carried out using three proportions of AC: P25: TiO_2 (synthesized), maintaining a 4% Ag/TiO_2 ratio. In a 500 mL beaker, 8.58 mL of titanium isopropoxide (TTIP) and 43.0 mL of 2-propanol were added and stirred for 30 min at 300 rpm. Then, 3.68 mL of hydrochloric acid was added dropwise. In a 250 mL Erlenmeyer flask, 0.302 g of silver nitrate was dissolved in 191.0 mL of water using a magnetic stirrer, covering the beaker to prevent the formation of silver oxide. To the stirred solution, AC and 2.4 g of P25 were added together with the nitrate solution. Finally, 2.0 M sodium hydroxide was added until pH 3 (approximately 18 mL) and left in stirring at 600 rpm for 5 h.

After the 5 h, the solution was washed by vacuum filtration until pH 7 was obtained in the filtered water. The wet gel was dried for 24 h at 80 °C and calcined for 3 h at 400 °C under a nitrogen atmosphere.

The amounts of AC used for the different proportions are shown in Table 1. The amounts of the other reagents were kept constant for all three catalysts.

2.6 Characterization of Activated Carbon and Catalysts

The scanning electron microscopy (SEM) images were performed on a ZEISS Merlin VP Compact model that has a BRUKER model Quantax 4000 EDX microanalysis system.

Table 1 Amount of CA used in different ratio

Reactivate	FCAg1 (1:1:1 ratio)	FCAg2 (ratio 1:0.6:0.6)	FCAg3 (ratio 1:0.2:0.2)
Activated carbon (g)	2.4	4.0	12.0

Transmission electron microscopy (TEM) was carried out on a JEOL model JEM-2010. This microscope has an OXFORD brand X-ray detector model INCA Energy TEM 100 for microanalysis (EDS). The image acquisition camera is from the GATAN brand, model ORIUS SC600, it is mounted on the axis with the microscope at the bottom and is integrated into the GATAN Digital Micrograph 1.80.70 image acquisition (Table 2).

The X-ray diffraction analysis was performed on a Bruker D8-Advance that has a KRISTALLOFLEX K 760-80F X-ray generator (power: 3000 W, voltage: 20–60 kV and current: 80 mA) with an RX tube with copper anode.

For the FTIR analysis, an Agilent model Cay 630 brand FTIR spectrometer was used, with MicroLab data processing software.

Diffuse reflectance spectroscopy was performed on a Jasco V-670, dual-beam UV–Vis/NIR spectrometer with wavelength range 190 to 2700 nm. The equipment has 2 lamps, one of deuterium (190 to 350 nm), and one halogen lamp (330 to 2700 nm).

The thermogravimetric analysis was carried out on a simultaneous TG–DTA unit of the METTLER TOLEDO brand, model TGA/SDTA851e/SF/1100. The gas used was a mixture of nitrogen and air.

2.7 Evaluation of Photocatalytic Activity

An ibuprofen solution of 15 ppm was prepared, then it was placed in ultrasound and heating (40 °C) for 2 h to improve the solubility, later, the pH was adjusted to 3.0 or 7.0 with HCl and/or NaOH 2.0 M. 300.0 mL of the solution was taken and transferred to the reactor. The system was stirred at 300 rpm. A bubbling system was set up to inject oxygen from the air. The reactor was placed in a jacket in which water circulates to maintain the temperature at 20.0 °C. The catalyst was added just before the tests. The reaction was carried out for 3 h. The amount of catalyst added was fixed to have a TiO_2 charge of 0.02% in the solution.

2.8 Quantification of Ibuprofen

Quantification of ibuprofen was performed using high-performance liquid chromatography (HPLC), a mixture of acetonitrile and phosphate buffer was used as the mobile phase in a ratio of 35:65, respectively, the mobile phase flow was 0.7 mL/min. For this case, a Merk brand C18 column and a

Journal : Large 11244 | Article No : 1311 | Pages : 14 | MS Code : 1311 | Dispatch : 4-7-2020

Table 2 Elemental composition—EDX report

Component	FCAg1 (1:1:1)		FCAg2 (1:0.6:0.6)		FCAg3 (1:0.2:0.2)	
	% w/w	Atomic %	% w/w	Atomic %	% w/w	Atomic %
C	82.34	89.03	87.77	93.74	89.65	93.55
Ti	4.64	1.26	2.71	0.72	1.22	1.22
Ag	0.19	0.02	0.77	0.09	0.19	0.02
O	10.84	8.80	4.78	3.84	6.52	5.10
Al	0.06	0.03	0.11	0.05	0.10	0.05
Si	0.61	0.28	0.36	0.16	0.38	0.17
S	0.93	0.38	2.84	1.14	1.77	0.69

UV/vis detector were used and configured at a wavelength of 222 nm. 60 L of previously filtered sample was injected into the chromatograph on 0.22 µm [33].

3 Results and Discussion

3.1 Activated Carbon

The specific surface area of AC obtained in the present study was 141.0 m^2/g, that is within the range reported in literature: 19.55 m^2/g [34] to 358.5 m^2/g [35].

Proximate analysis of AC showed a moisture content of 0.6%, consistent with the results from previous works [36]. Besides, the AC presented ash contents of 16.0%, volatile matter of 5.7%, and fixed carbon of 77.7% on a wet basis. The content of volatile matter depends dramatically on carbonization and activation time. The temperature at which these treatments are carried out ranges between 400 and 1000 °C, removing organic molecules from carbonaceous material. Before carbonization, the content of volatile matter ranges between 50 and 80% [37], and decreases to values between 3 and 7% after activation. The amount of fixed carbon is high compared to ACs obtained with similar procedures, where it is generally between 44 and 18% for treatments of 1 to 3 h respectively, decreasing as time increases [36]. The high fixed carbon content may be related to differences in the characteristics of the rubber used, which can produce materials with different thermogravimetric behavior [38]. The burn-off of the AC is 85%, which increase the surface area of the material with the increase in burn-off [39]. A high burn-off can benefit the photocatalytic process; the burn-off achieved is higher than in other works by about 5%, where pyrolysis was carried out in the same way and activation was carried out only for 2 h under the same conditions, this higher burn-off in the present work is related to the longer activation time used, one hour more than the residence time reported by Torikai and coworkers, wich increases the quantity of volatile matter removed from the carbonaceos material bringing a higher burn-off [40].

3.2 Characterization

3.2.1 SEM and EDX

Figure 2 shows the SEM images where it can be seen that AC without the addition of titanium or silver has completely uniform coral morphology. This morphology is characteristic of the type of precursor and agrees with previous studies [33, 41]. In the first work, the activation was done with N_2 and steam, while in the second one, the activation process is carried out the same as the present work, with the difference that they used a 2 h activation time instead of 3. For Fig. 2b, the presence of some light areas in the micrograph can be noted, which are associated with agglomerates of inorganic matter. In the 2c, the number and size of these agglomerates increases, presenting some white crystals, and finally, the sample with the highest content of titanium, 2d, presents a high agglomeration of particles of inorganic matter with gray and white colorations, as can be seen from the EDX mapping. This mapping also shows that both, silver and titanium particles, are heterogeneously dispersed. The amount of silver that is added affects crystal growth and it has been shown that higher silver contents generate agglomeration and a larger particle size [21]. This behaviour was studied by Mogal and colaborators, where they found that the amount of silver affects directly the crystallites/particle growth and aggregation [42]. This is by repulsion between crystallites/particles due to the presence of doped silver ions of electropositive nature. It is also affected by the size of Ag^+ ions, since they cannot enter the TiO_2 lattice and therefore agglomerate at the surface**.** When comparing with SEM images of previous works [12] the disposition and morphology corresponds to the anatase phase of TiO_2.

From the EDX analysis, the mapping shows that the titanium and silver particles in green and red respectively (Fig. 3b, d, f) are scattered. In the catalysts with the highest and lowest titanium content, it is identified that the carbon content increases, titanium decreases, and silver is constant as expected, except for a higher content of Ag in catalyst 2, this probably due to the mapping it was carried out in a zone of high aggeration of the element. Likewise, a high sulfur

Journal : Large 11244 | Article No : 1311 | Pages : 14 | MS Code : 1311 | Dispatch : 4-7-2020

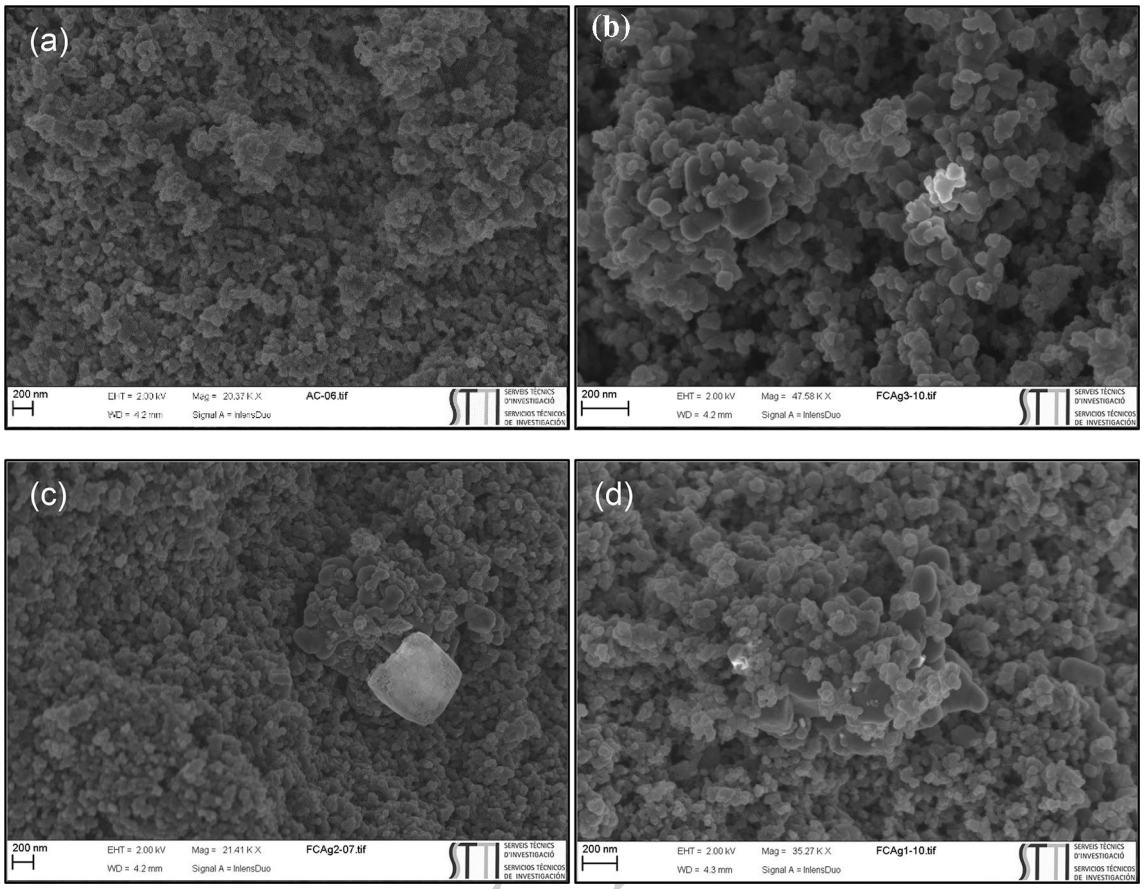

Fig. 2 Scanning electron microscopy. **a** AC, **b** FCAg3, **c** FCAg2, **d** FCAg1

content was found due to the origin of the carbon precursor (rim rubber). The oxygen content of the samples increases with increasing TiO_2 content, indicating that it is mainly the oxygen from this oxide. The other compounds such as Si, Na, Cl, are mainly attributed to components of the inorganic matter of tire rubber used as a precursor of AC, and to residues of reagents used in the synthesis of catalysts.

3.2.2 TEM

Figure 4 shows the TEM analyzes, in which the presence of silver nanoparticles and TiO_2 is observed. Titanium nanoparticles are round in shape and partially agglomerated with an average particle size of 76 × 25.3 nm. The average particle size of the catalysts obtained is greater than the average particle size of TiO_2 P25, which is between 10 and 30 nm [43]. This is attributed that as the concentration of TiO_2 increases, the precursor finds no silver surfaces available for nuclear and self-aggregation, leading to the formation of larger particles [44].

Particle size analysis was carried out using ImageJ software, 122 particles were taken and the results were fitted to a Gaussian distribution with an R^2 0.88, mean value of 75.58 nm and standard deviation 50.59 nm (Fig. 5).

3.2.3 X-ray Diffraction—XRD

Figure 6 shows the XRD patterns for the synthesized catalysts. All the catalysts show diffraction peaks at 25.3°, 37.8°, 48.0°, 53.8°, 54.9° and 62.8° that belong to the cristal plans (101), (004), (200), (105), (211) and (204) of anatase. Also, diffraction peaks at 27.5°, 36.1°, 41.2°and 54.3° corresponding to the crystal plans (110), (101), (111), and (211) of rutile [45]. Only, the FCAg3 catalyst showed diffraction peaks for metallic silver at 38.1°, 44.3°, 64.4°, and 77.4° [19] diffraction plans (111), (200), (220) and (311). Finding metallic silver only in the FCAg3 catalyst can be explained by the homogeneous dispersion of the metallic compound in the catalyst, nevertheless, the presence of the compound was in the three obtained catalysts by the EDX analysis.

Although it has been shown that pure anatase has greater catalytic activity than rutile, it is recognized that anatase/rutile mixtures show synergistic effects, which increase photocatalytic activity, due to the reduction in electron/hole pair recombination [46]. The average intensity of the main

Journal : Large 11244 | Article No : 1311 | Pages : 14 | MS Code : 1311 | Dispatch : 4-7-2020

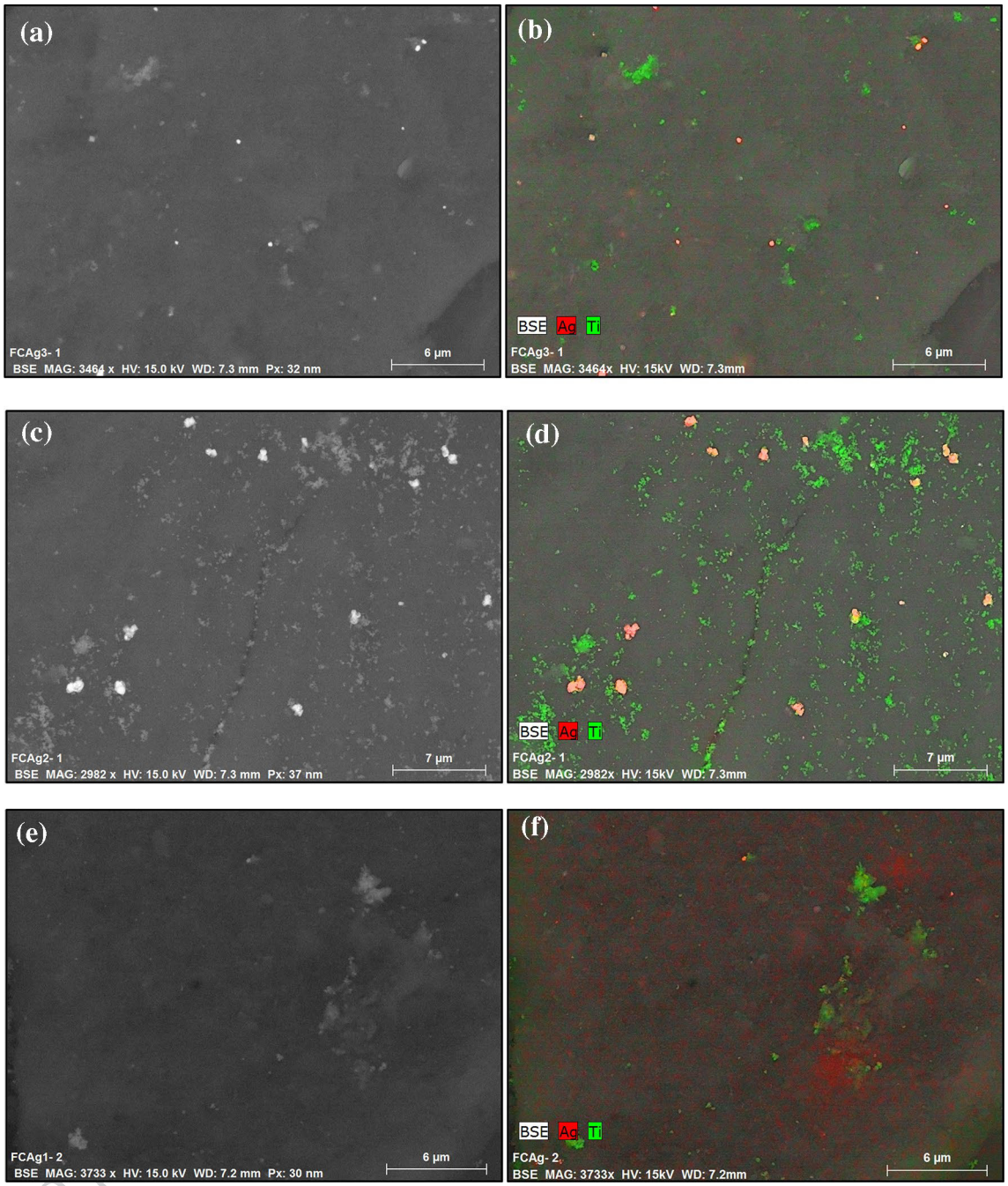

Fig. 3 EDX mapping, **a** FCAg3 micrograph, **b** FCAg3 mapping, **c** FCAg2 micrograph, **d** FCAg2 mapping, **e** FCAg1 micrograph, **b** FCAg1 mapping

peak for the rutile phase is considerably lower than the average intensity of the main peak for the anatase phase, which indicates that all catalysts have a higher proportion of TiO_2 in the anatase phase. Also, TiO_2 peaks in both anatase and rutile phase decreased as the proportion of this decreased in the catalysts. The average anatase crystallite sizes of each prepared catalyst are tabulated in Table 3 and were calculated using the Debye-Scherer equation with a K constant of 0.94, a wavelength of X-Ray of 0.15406 nm and full width at half-maximum of the (101) reflection at 25.3°.

Photocatalysis is essentially a surface phenomenon, therefore its efficiency is influenced by the particle size of the catalyst; lower particles favor the process [47] and result in higher surface areas, so the photocatalytic activity of the catalysts obtained should be greater than that of the commercial TiO_2 Degussa P25 which generally has a crystallite size

Journal : Large 11244 | Article No : 1311 | Pages : 14 | MS Code : 1311 | Dispatch : 4-7-2020

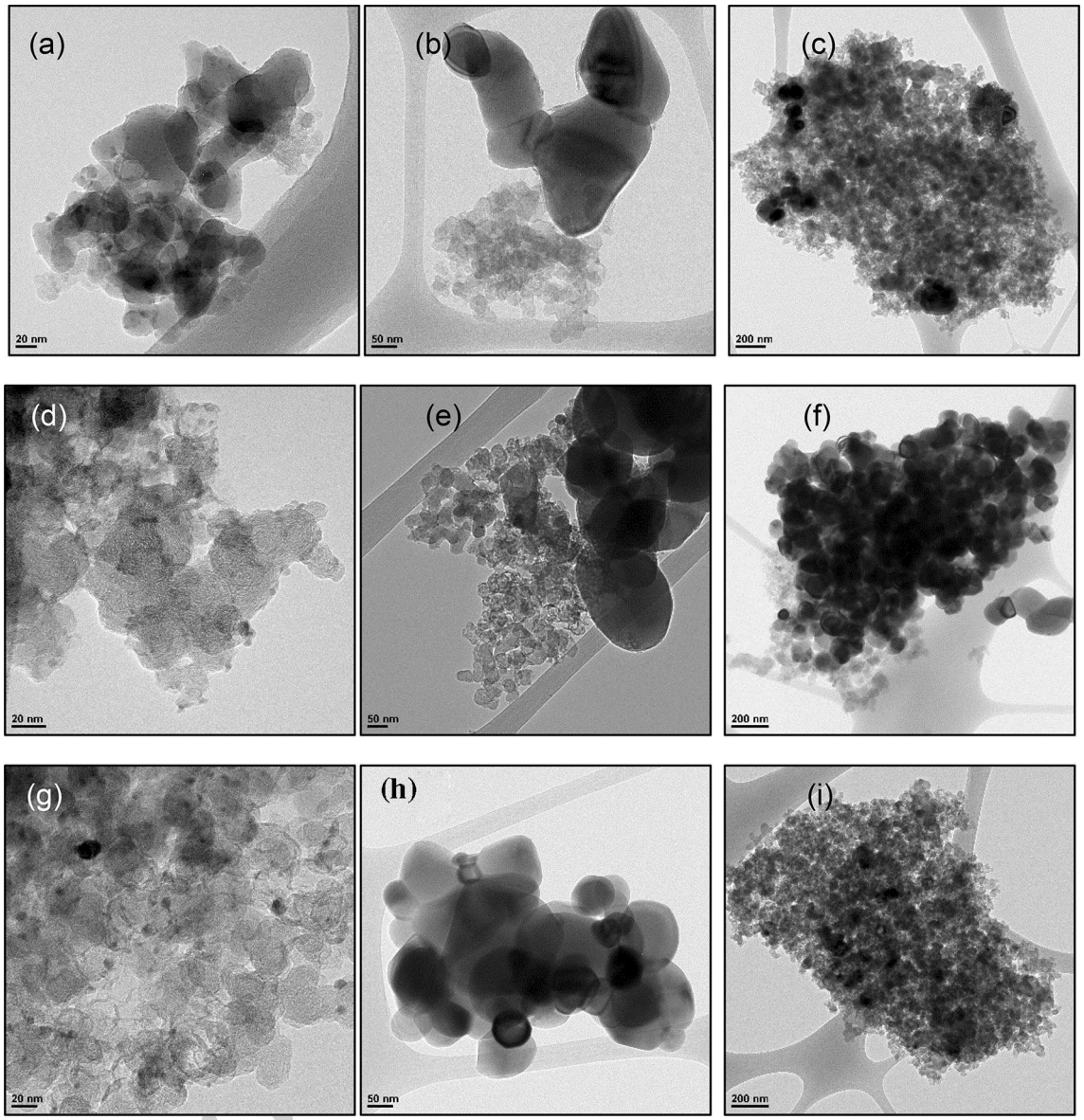

Fig. 4 Transmission electron microscopy **a** FCAg1 20 nm, **b** FCAg1 50 nm, **c** FCAg1 200 nm, **d** FCAg2 20 nm, **e** FCAg2 50 nm, **f** FCAg2 200 nm, **g** FCAg3 20 nm, **h** FCAg3 50 nm, **i** FCAg3 200 nm

around 40 nm [46]. The structure of the catalysts is mainly composed of TiO_2 in the anatase phase and the crystal sizes of the catalysts are in the general range of 14–50 nm [47].

3.2.4 Infrared Spectroscopy—FTIR

Figure 7 shows the results obtained from the FTIR analysis. Bands between 1800 and 2400 cm^{-1} are characteristic of AC, and, as this is the support material for the photocatalytic components, they are preserved after the synthesis and calcination process of each catalyst. The strong band exhibited close to 2169 cm^{-1} corresponds to the vibrations of the asymmetric CO_2 stretch [46, 48] used in physical activation. The pronounced bands on the catalysts at 1040 cm^{-1} corresponds to the Ti–O–C bond that indicates the conjugation between titanium and AC, and the bands between 400 and 800 cm^{-1} represent the Ti–O bond [12]. When comparing the different spectra, it is evident that as the carbon content increases, the Ti-OC band trends to decrease because of the carbonaceous precursor. Spectra do not show bands at 3809, 3415 cm^{-1}, which corresponds to the stretching of hydroxyl groups (–OH) [46, 49] indicating the absence of adsorbed water and hydroxyl groups in the catalysts.

Journal : Large 11244 | Article No : 1311 | Pages : 14 | MS Code : 1311 | Dispatch : 4-7-2020

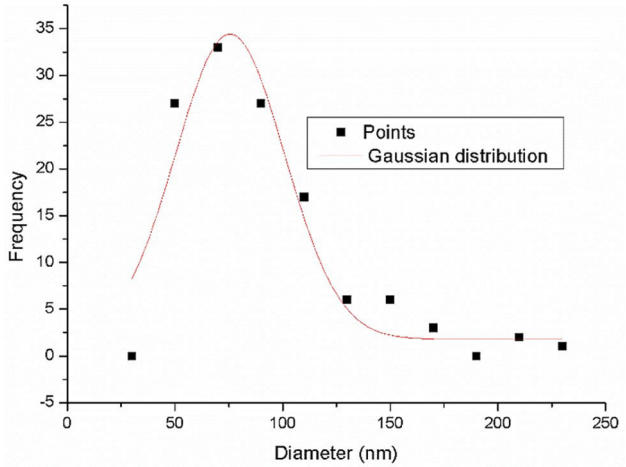

Fig. 5 Particle size distribution

3.2.5 UV/Vis Diffuse Reflectance Spectroscopy

Figure 8 shows the results of the diffuse reflectance analysis of the catalysts. The spectra share the absorption region between 200 and 380 nm that corresponds to the absorption region of titanium dioxide. On the spectrum for TiO_2 reported previously [50] absorbing at wavelengths greater than 380 nm. In this case, after that wavelength, a lower absorption in the visible spectrum is seen. The bands observed between 400 and 800 nm correspond to the combined effect of photon absorption by AC and the presence of metallic silver [21, 23] identified in the XRD analysis. The spectra of the FCAg1 and FCAg2 catalysts show similarities, however, the FCAg3 catalyst, which is the one with the lowest content of TiO_2 and Ag, presented a higher absorbance indicating a better interaction with radiation in this material; from the EDX analysis it is evident that the amount of silver present is the same in the catalysts, however, when observing the SEM mappings and images, it is clear that the FCAg3 catalyst has a more homogeneous distribution.

Bandgap of the catalyst was calculated using the Kubelka Munk equation, which assumes that incident irradiation on a dispersing medium goes under simultaneous absorption and dispersion processes. The reflected irradiation can be expressed as a function of the absorption (k) and dispersion (S) constants, as shown in Eq. 1.

Table 3 Average crystallite size of the prepared catalysts

Catalysts	Average crystallite size (nm)	Standar deviation (nm)
FCAg1 (1:1:1)	28.36	3.58
FCAg2 (1:0.6:0.6)	26.06	2.17
FCAg3 (1:0.2:0.2)	32.94	0.85

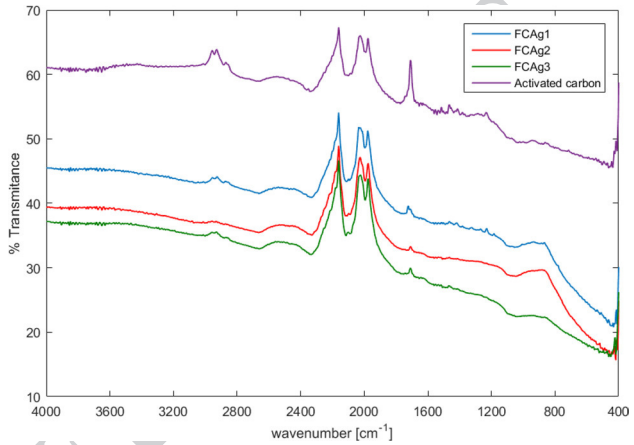

Fig. 7 FTIR spectra for the materials

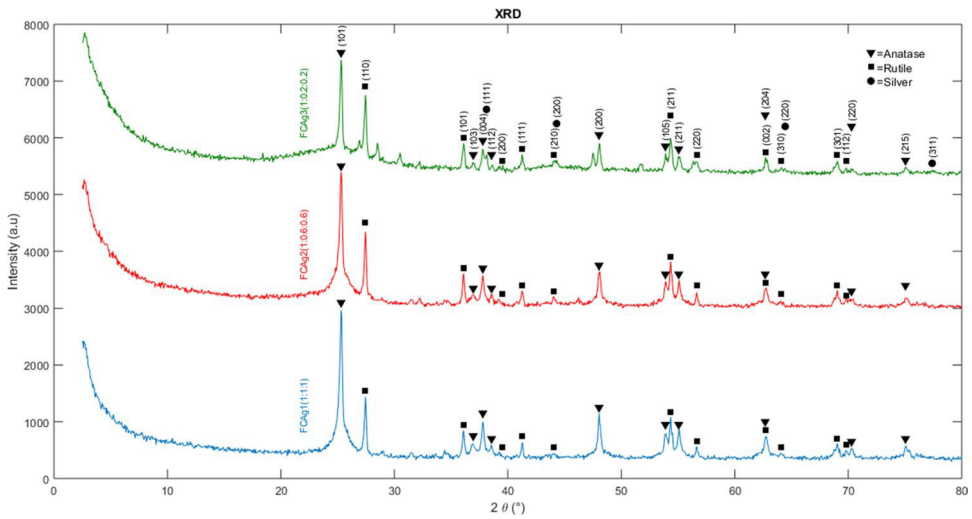

Fig. 6 XRD pattern of FCAg1, FCAg2, FCAg3

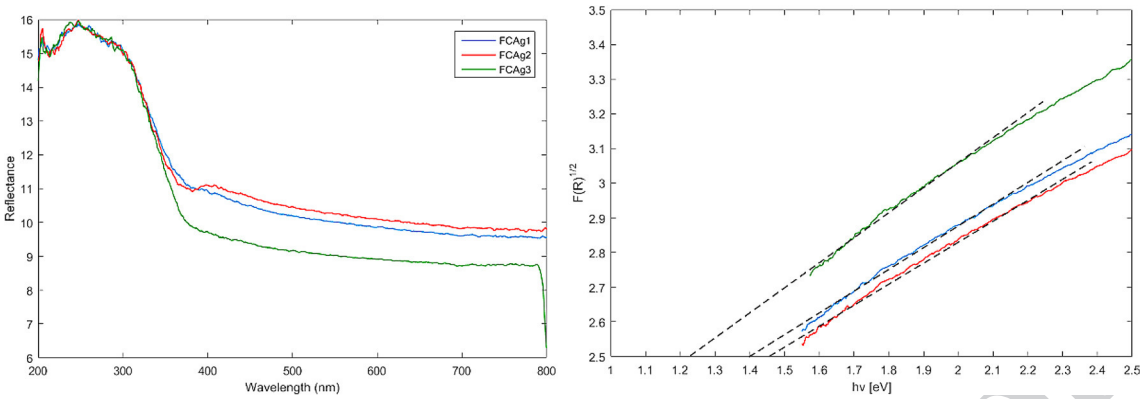

Fig. 8 UV–Vis diffuse reflectance spectrum

$$F(R) = \frac{\left(1 - R_\infty\right)^2}{2R_\infty} = \alpha \quad (1)$$

where $F(R)$ is the Kubelka–Munk function corresponding to the absorbance, R_∞ is the reflectance of an infinitely thick sample with respect to a reference at each wavelength, and, α is the linear absorption coefficient of the material.

The energy of incident photons and energy of the optical band gap of the material can be related by Eq. 2.

$$\alpha \cdot h\nu = C\left(h\nu - E_g\right)^n \quad (2)$$

where h is Planck's constant (4.136×10^{-15} eVs^{-1}), C is an energy independent constant, $h\nu$ is the photon energy (eV), E_g is the optical band gap energy (eV), and n is a constant that determines the type of optical transition. For this case we considered n = 1/2 as suggested in previous studies [51]. The value of the band gap was obtained from a tangent line to the $[F(R)h\nu]^{1/n}$ vs $h\nu$ curve as is shows in the Fig. 8.

The reported value for TiO_2 is 3.2 eV [19]. As shown in Table 4, the FCAg3 catalyst has the lowest prohibited band with 1.23 eV, while the other 2 catalysts have similar bands, from this it is evident that the AC:TiO_2:Ag 1:0.2:0.2 present the best combination since it achieves the greatest reduction of the prohibited band.

3.2.6 Thermogravimetry

As it is shown in Fig. 9 between 20 and 90 °C there are no changes larger than 1% for all samples, indicating that catalysts and AC do not have significant moisture content [48]. The loss of mass in both AC and catalysts between 419 and 616 °C is attributed to the oxidation of AC in this temperature range as well as the phase change from anatase to rutile [46]. When comparing the curves, it is observed that the lower the carbon content in the sample, the loss of mass in this interval is less; AC loses approximately 80% of the mass and the FCAg3, FCAg2 and FCAg1 catalysts lose 57, 39 and 24% respectively.

Table 4 Band gap of catalysts

Catalyst	Band gap (eV)
FCAg1	1.40
FCAg2	1.48
FCAg3	1.23

The mass that remains almost constant after 616 °C is attributed to silver, titanium dioxide, and AC ash. According to the TG-TGA analysis carried out on AC, it is possible to determine that the ash content is 16.28%. This result varies by only 1.7% compared to the value obtained in the proximate analysis.

3.3 Evaluation of Photocatalytic Activity

Figures 10 and 11 show the results of the ibuprofen removal with the different catalysts and UV and visible light. From the pH conditions evaluated, it was evident that the best condition for the photocatalytic process occurs at pH 3, and it was also observed that at such pH, with the FCAg3 using visible light, the maximum removal of ibuprofen occurs, as was seen in the diffuse reflectance spectrum, the FCAg3 catalyst shows the highest absorbance in the visible spectrum, also, this material has the lowest prohibited band of the three catalysts. Morphological characterizations showed that both titanium and silver nanoparticles are dispersed more homogeneously than in the other 2 catalysts, allowing better adsorption and contact with photocatalytic components.

The presence of silver and carbon significantly affects the properties of doped TiO_2 photocatalyst, mainly increases the adsorption capacity, disperses the active phase, and decreases the band gap. The FCAg3 catalyst was the most efficient photocatalyst showing the best physical–chemical properties. Similar relations between physical–chemical

Journal : Large 11244 | Article No : 1311 | Pages : 14 | MS Code : 1311 | Dispatch : 4-7-2020

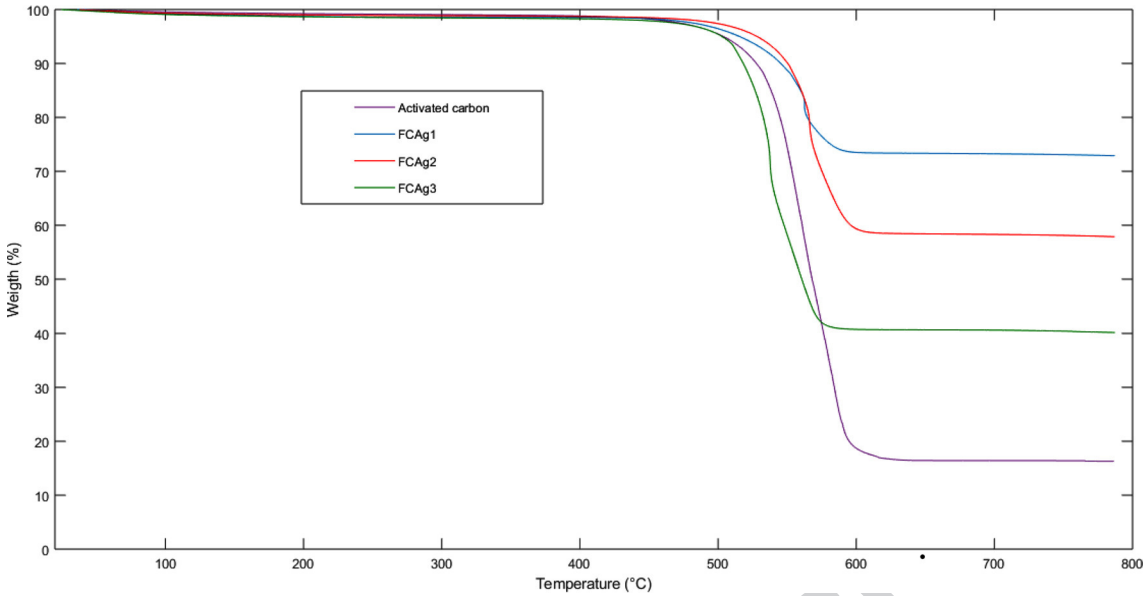

Fig. 9 Thermogravimetric analysis

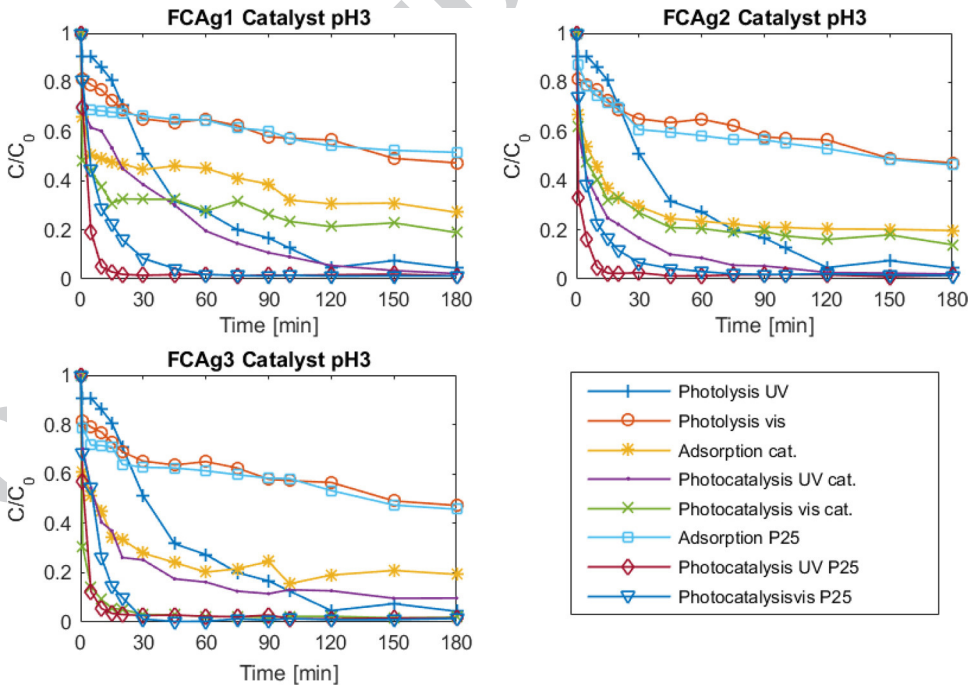

Fig. 10 Kinetics of removal of ibuprofen with the different catalysts at pH 3

characteristics have been obtained for other systems. Homogeneous dispersion of the titanium dioxide and silver in the support improves the catalytic efficiency, increasing the number of active sites for the phtocatalytic reactions. For instance, Mogal and colaborators established that the optimum amount of silver (0.75 at.%) effectively controls the particle growth and agglomeration, surface area, thermal stability, band gap on photocatalytic activity in phthalic acid [21]. Sanzone found that the enhancement of the activity towards the discoloration of methylene blue, using Ag nanoparticles embedded in a TiO_2 thin film, with visible light is strictly related to the intensity of the field at the surface and to the presence of silver NPs (Plasmonic metal nanoparticles) [52]. Cui and colaborators agreed that Fe-doped TiO_2 on hollow glass microbeads increases the photocatalytic efficiency of oxidation of methyl orange, due to the recombination centers for the photogenerated carriers [53]. Peñas in a recent work tested several ACs (from lignin) for

Journal : Large 11244 | Article No : 1311 | Pages : 14 | MS Code : 1311 | Dispatch : 4-7-2020

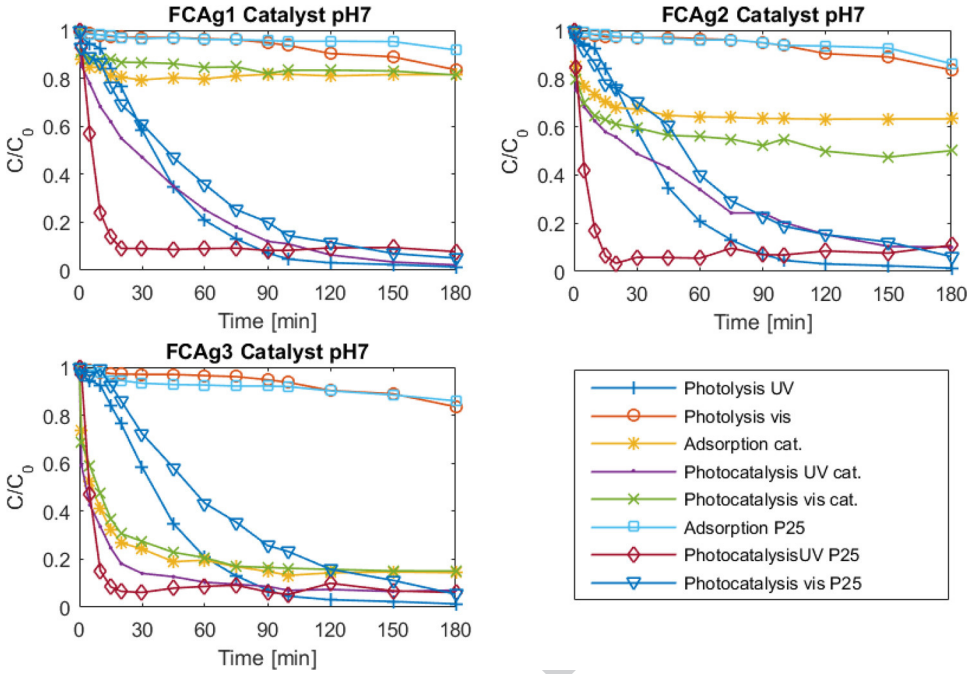

Fig. 11 Kinetics of removal of ibuprofen with the different catalysts at pH 7

preparing the TiO_2/AC heterostructures for photocatalytic treatment of acetaminophen, finding that properties and activity depended on the chemical compound that was used to activate the lignin and that the catalyst conformed by TiO_2/Fe–C showed the best efficiency under solar-simulated irradiation [54].

The relation between anatase and rutile phases and its effect on the photocatalytic reactions have been studied extensively [55, 56]. The intimate contact among the amorphous, anatase, and rutile TiO_2 was believed to improve the magnitude of the space-charge potential due to the efficient charge carrier separation, leading to a much higher photocatalytic activity than that of sole-phase TiO_2. The interface of anatase–rutile nanoparticles, like the heterojunction structure, is beneficial to the charge carrier separation and consequently the efficiency of photocatalysis [20]. The role of the silver in the catalyst is of an electron–hole mediation, avoiding the recombination of the electron–hole pair. Also, a plasmonic effect is obtained with the addition of silver to the catalyst.

From the analysis of the kinetics obtained with the different catalysts, it is evident that pH has a significant effect on the process and it is clear that acidic pH tends to favor the process. It was observed that adsorption was favored at pH 3 for FCAg1 and FCAg2; at this pH, lower than the pKa of the ibuprofen (4.91 [57]) the molecule is protonated being neutral, while at pH 7 de molecule is deprotonated forming an anion, then the increase of adsorption at lower pH suggest a posible repulsion of the molecule with negative charges of the surface of the catalysts at pH 7 [10]. In the case of FCAg3 the adsorption is similar at both pH. Nevertheless, FCAg3 at pH 3 has a better behavior for the removal of ibuprofen compared with P25 under visible radiation.This migh be due to the reduction of the band gap energy for the syntetized catlyst that improves the photocatalytic reactions added to the adsorption on the surface of the AC.

Regarding the contributions of the different effects of adsorption, photolysis, and photocatalysis, it is observed that in the presence of UV radiation, the photolysis almost completely degrades ibuprofen, however, in the presence of visible light, this effect does not contribute significantly.

4 Conclusions

The FCAg3 catalyst has the best performance in the presence of UV and visible radiation and pH 3 for the degradation of ibuprofen, because it shows a greater dispersion of titanium, which allows a better distribution of radiation, as evidenced in the analysis of spectroscopy since this catalyst has a higher absorbance. pH is a determining factor in the photocatalytic process and, as seen at low pH, adsorption is favored in FCAg1 and FCAg2, while photocatalysis is favored in FCAg3.

The characterizations carried out showed that the catalysts present an agglomeration of titanium particles, as well as that the surface of the AC support presents a coral morphology. From the EDX analyzes the presence of metallic silver and the rutile and anatase phases of titanium were found. Spectroscopy analysis shows that the lower the amount of titanium, the greater the absorbance in the visible spectrum, as well as a decrease in the titanium bandgap.

Journal : Large 11244 | Article No : 1311 | Pages : 14 | MS Code : 1311 | Dispatch : 4-7-2020

From the thermogravimetric analysis, a greater loss of mass was observed when the carbon decomposes and the phase change in the titanium occurs.

The ratio of titanium and AC is of great importance and influences the efficiency of the process. It was evidenced that the lower ratio in titanium allows a greater degradation in the visible spectrum in acid pH condition.

Acknowledgements The authors would like to thank to Automundial for the rubber supply. The DICE of the Universidad Jorge Tadeo Lozano for the financial support, and Andrea Alvarez and Felipe Mendoza for their assistance in the analytical methods.

References

1. Candido JP, Andrade SJ, Fonseca AL et al (2017) Ibuprofen removal by heterogeneous photocatalysis and ecotoxicological evaluation of the treated solutions. Environ Sci Pollut Res. https://doi.org/10.1007/s11356-017-8623-3
2. Carter WC, Brown BR (2013) Ibuprofen: clinical pharmacology, medical uses and adverse effects. Nova Science Publishers, New York
3. Lambropoulou DA, Nollet LML (2014) Transformation products of emerging contaminants in the environment. Wiley, West Sussex
4. Janet Gil M, María Soto A, Iván Usma J, Darío Gutiérrez O (2012) Emerging contaminants in waters: effects and possible treatments. Prod + Limpia 7:52–73
5. Carr DL, Morse AN, Zak JC, Anderson TA (2011) Biological degradation of common pharmaceuticals and personal care products in soils with high water content. Water Air Soil Pollut. https://doi.org/10.1007/s11270-010-0573-z
6. Bu Q, Shi X, Yu G et al (2016) Assessing the persistence of pharmaceuticals in the aquatic environment: challenges and needs. Emerg Contam. https://doi.org/10.1016/j.emcon.2016.05.003
7. Carr DL (2010) Biotransformation of pharmaceuticals and personal care products (PPCPs) at an effluent land application site
8. Araujo L, Troconis M, Espina M, Prieto A (2014) Persistence of ibuprofen, ketoprofen, diclofenac and clofibric acid in natural waters. J Environ Hum. https://doi.org/10.15764/eh.2014.02005
9. Puszkarewicz A, Kaleta J, Papciak D (2017) Application of powdery activated carbons for removal ibuprofen from water. J Ecol Eng 10:20. https://doi.org/10.12911/22998993/74289
10. Mestre AS, Pires J, Nogueira JMF, Carvalho AP (2007) Activated carbons for the adsorption of ibuprofen. Carbon. https://doi.org/10.1016/j.carbon.2007.06.005
11. Lach J, Szymonik A, Ociepa-Kubicka A (2018) Adsorption of selected pharmaceuticals on activated carbons from water. In: E3S web of conferences. pp 1–8
12. Tran TTH, Kosslick H, Schulz A, Nguyen QL (2017) Photocatalytic performance of crystalline titania polymorphs in the degradation of hazardous pharmaceuticals and dyes. Adv Nat Sci Nanosci Nanotechnol. https://doi.org/10.1088/2043-6254/aa5956
13. Murcia JJ, Hernández JS, Rojas H et al (2020) Evaluation of Au–ZnO, ZnO/Ag_2CO_3 and Ag–TiO_2 as photocatalyst for wastewater treatment. Top Catal. https://doi.org/10.1007/s11244-020-01232-z
14. Talat-Mehrabad J, Khosravi M, Modirshahla N, Behnajady MA (2016) Synthesis, characterization, and photocatalytic activity of co-doped Ag-, Mg-TiO_2-P25 by photodeposition and impregnation methods. Desalin Water Treat. https://doi.org/10.1080/19443994.2015.1036780
15. Singh P, Vishnu MC, Sharma KK et al (2016) Comparative study of dye degradation using TiO_2-activated carbon nanocomposites as catalysts in photocatalytic, sonocatalytic, and photosonocatalytic reactor. Desalin Water Treat. https://doi.org/10.1080/19443994.2015.1108871
16. Habibi MH, Nasr-Esfahani M (2008) Silver doped TiO_2 nanostructure composite photocatalyst film synthesized by sol-gel spin and dip coating technique on glass. Int J Photoenergy. https://doi.org/10.1155/2008/628713
17. Cojocaru B, Neaţu Ş, Pârvulescu VI et al (2009) Synergism of activated carbon and undoped and nitrogen-doped TiO_2 in the photocatalytic degradation of the chemical. Warfare agents Soman, VX, and Yperite. Chem Sustain Energy Mater. 10:20. https://doi.org/10.1002/cssc.200800246
18. Hammer N, Mathisen K, Rønning M (2013) CO oxidation over Au/TiO_2-carbon catalysts: the effect of thermal treatment, stability and TiO_2 support structure. Top Catal. https://doi.org/10.1007/s11244-013-0023-4
19. El SI, Erdei L, Shon HK, Kim JH (2011) Development of visible light sensitive titania photocatalysts by combined nitrogen and silver doping. J Ind Eng Chem. https://doi.org/10.1016/j.jiec.2011.02.039
20. Jiang X, Manawan M, Feng T, Qian R, Zhao T, Zhou G, Kong F, Wang Q, Dai S, Pan JH (2018) Anatase and rutile in evonik aeroxide P25: heterojunctioned or individual nanoparticles? Catal Today. https://doi.org/10.1016/j.cattod.2017.06.010
21. Mogal SI, Gandhi VG, Mishra M et al (2014) Single-step synthesis of silver-doped titanium dioxide: influence of silver on structural, textural, and photocatalytic properties. Ind Eng Chem Res. https://doi.org/10.1021/ie404230q
22. Li LC, Tseng YH, Lin H (2020) Efficient photodecomposition of NOx on carbon modified Ag/TiO_2 nanocomposites. Top Catal. https://doi.org/10.1007/s11244-020-01255-6
23. Likun G, Wentao G, Shaoliang X et al (2015) Enhancement of photo-catalytic degradation of formaldehyde through loading anatase TiO_2 and silver nanoparticle films on wood substrates. RSC Adv. https://doi.org/10.1039/C5RA06390F
24. Keane D (2013) Evaluation of the performance of activated carbon and titanium dioxide composites for pharmaceutical adsorption and photocatalysis in water. Dublin City University, Dublin
25. Hench LL, West JK (1990) The sol–gel process. Chem Rev. https://doi.org/10.1021/cr00099a003
26. Belgacem A, Belmedani M, Rebiai R, Hadoun H (2013) Characterization, analysis and comparison of activated carbons issued from the cryogenic and ambient grinding of used tyres. Chem Eng Trans. https://doi.org/10.3303/CET1332285
27. Sofi A (2018) Effect of waste tyre rubber on mechanical and durability properties of concrete: a review. Ain Shams Eng J. https://doi.org/10.1016/j.asej.2017.08.007
28. Wik A (2007) Toxic components leaching from tire rubber. Bull Environ Contam Toxicol. https://doi.org/10.1007/s00128-007-9145-3
29. Reisman JI, Lemieux PM (1997) Air emissions from scrap tire combustion. US Environ Prot Agency, Off Res Dev
30. Dimpe KM, Ngila JC, Nomngongo PN (2017) Application of waste tyre-based activated carbon for the removal of heavy metals in wastewater. Cogent Eng. https://doi.org/10.1080/23311916.2017.1330912
31. Karmacharya MS, Gupta VK, Jha VK (2016) Preparation of activated carbon from waste tire rubber for the active removal of Cr(VI) and Mn(II) ions from aqueous solution. Trans Indian Ceram Soc. https://doi.org/10.1080/0371750X.2016.1228481
32. Li L, Liu S, Zhu T (2010) Application of activated carbon derived from scrap tires for adsorption of Rhodamine B. J Environ Sci. https://doi.org/10.1016/S1001-0742(09)60250-3

33. Papamija M, Sarria V (2010) Photocatalytic degradation of Ibuprofen using titanium dioxide. Rev Ing 31:47–53
34. Zabaniotou A, Madau P, Oudenne PD et al (2004) Active carbon production from used tire in two-stage procedure: industrial pyrolysis and bench scale activation with H_2O-CO_2 mixture. J Anal Appl Pyrolysis. https://doi.org/10.1016/j.jaap.2004.08.002
35. Loloie Z, Mozaffarian M, Soleimani M, Asassian N (2017) Carbonization and CO_2 activation of scrap tires: optimization of specific surface area by the Taguchi method. Korean J Chem Eng. https://doi.org/10.1007/s11814-016-0266-4
36. Skodras G, Diamantopoulou I, Zabaniotou A, Stavropoulos G, Sakellaropoulos GP (2007) Enhanced mercury adsorption in activated carbons from biomass materials and waste tires. Fuel Process. Technol. https://doi.org/10.1016/j.fuproc.2007.03.008
37. Ucar S, Karagoz S, Ozkan AR, Yanik J (2005) Evaluation of two different scrap tires as hydrocarbon source by pyrolysis. Fuel. https://doi.org/10.1016/j.fuel.2005.04.002
38. Martínez Hernández B, Viola DDJ, Solano SB, Polo EP (2016) Desvulcanización del caucho de neumáticos descartados aplicando XILOL asistido por microondas. https://doi.org/10.13140/RG.2.1.4420.5048
39. Teng H, Serio MA, Whjtowicz MA et al (1995) Reprocessing of used tires into activated carbon and other products. Ind Eng Chem Res 34:3102–3111
40. Torikai N, Meguro TN (1979) Pore size distribution of activated carbons made from tires which contain carbon blacks differing in particle size. Nippon Kagaku Kaishi 11:1604–1608
41. Murillo R, Navarro MV, García T et al (2005) Production and application of activated carbons made from waste tire. Ind Eng Chem Res. https://doi.org/10.1021/ie050506w
42. Mogal SI, Gandhi VG, Mishra M, Tripathi S, Shripathi T, Joshi PA, Shah DO (2014) Single-step synthesis of silver-doped titanium dioxide: influence of silver on structural, textural, and photocatalytic properties. Ind Eng Chem Res. https://doi.org/10.1021/ie404230q
43. Choina J, Kosslick H, Fischer C et al (2013) Photocatalytic decomposition of pharmaceutical ibuprofen pollutions in water over titania catalyst. Appl Catal B Environ. https://doi.org/10.1016/j.apcatb.2012.09.053
44. Angkaew S, Limsuwan P (2012) Preparation of silver-titanium dioxide core-shell (Ag@TiO2) nanoparticles: effect of Ti-Ag mole ratio. Procedia Eng. https://doi.org/10.1016/j.proeng.2012.01.1322
45. Oh WC, Zhang FJ, Chen ML et al (2009) Characterization and relative photonic efficiencies of a new Fe-ACF/TiO_2 composite photocatalysts designed for organic dye decomposition. J Ind Eng Chem. https://doi.org/10.1016/j.jiec.2008.09.019
46. Rosa SMC, Nossol ABS, Nossol E et al (2017) Non-synergistic UV-A photocatalytic degradation of estrogens by nano-TiO_2 supported on activated carbon. J Braz Chem Soc. https://doi.org/10.5935/0103-5053.20160201
47. Alzamani M, Shokuhfar A, Eghdam E, Mastali S (2013) Influence of catalyst on structural and morphological properties of TiO_2 nanostructured films prepared by sol–gel on glass. Prog Nat Sci Mater Int. https://doi.org/10.1016/j.pnsc.2013.01.012
48. Xing B, Shi C, Zhang C et al (2016) Preparation of TiO_2/activated carbon composites for photocatalytic degradation of RhB under UV light irradiation. J Nanomater. https://doi.org/10.1155/2016/8393648
49. Araña J, Doña-Rodríguez JM, Tello Rendón E et al (2003) TiO_2 activation by using activated carbon as a support: part I. Surface characterisation and decantability study. Appl Catal B Environ. https://doi.org/10.1016/S0926-3373(03)00107-3
50. Martínez Martínez J, Murillo R, García T (2013) Production of carbon black from pyrolysis of used tires. Boletín del Grupo Español del Carbón 10–14
51. Velo-Gala I, López-Peñalver JJ, Sánchez-Polo M, Rivera-Utrilla J (2014) Surface modifications of activated carbon by gamma irradiation. Carbon. https://doi.org/10.1016/j.carbon.2013.09.087
52. Sanzone G, Zimbone M, Cacciato G, Ruffino F, Carles R, Privitera V, Grimaldi MG (2018) Ag/TiO_2 nanocomposite for visible light-driven photocatalysis. Superlattice Microst. https://doi.org/10.1016/j.spmi.2018.09.028
53. Cui L, Wang Y, Niu M, Chen G, Cheng Y (2009) Synthesis and visible light photocatalysis of Fe-doped TiO_2 mesoporous layers deposited on hollow glass microbeads. J Solid State Chem. https://doi.org/10.1016/j.jssc.2009.07.045
54. Peñas-Garzón M, Gómez-Avilés A, Bedia J, Rodriguez JJ, Belver C (2019) Effect of activating agent on the properties of TiO_2/activated carbon heterostructures for solar photocatalytic degradation of acetaminophen. Materials. https://doi.org/10.3390/ma12030378
55. Bickley RI, Gonzalez-Carreno T, Lees JS, Palmisano L, Tilley RJD (1991) A structural investigation of titanium dioxide photocatalysts. J Solid State Chem. https://doi.org/10.1016/0022-4596(91)90255-G
56. Ohno T, Sarukawa K, Tokieda K, Matsumura M (2001) Morphology of a TiO_2 photocatalyst (Degussa, P-25) consisting of anatase and rutile crystalline phases. J Catal. https://doi.org/10.1006/jcat.2001.3316
57. Lindqvist N, Tuhkanen T, Kronberg L (2005) Occurrence of acidic pharmaceuticals in raw and treated sewages and in receiving waters. Water Res. https://doi.org/10.1016/j.watres.2005.04.003

Journal : Large 11244 | Article No : 1311 | Pages : 14 | MS Code : 1311 | Dispatch : 4-7-2020

Journal:	**11244**
Article:	**1311**

Author Query Form

Please ensure you fill out your response to the queries raised below and return this form along with your corrections

Dear Author

During the process of typesetting your article, the following queries have arisen. Please check your typeset proof carefully against the queries listed below and mark the necessary changes either directly on the proof/online grid or in the 'Author's response' area provided below

Query	Details Required	Author's Response
AQ1	As per style, email ID is mandatory for the corresponding author. Author L. R. Conde-Rivera is mentioned with asterisk but email id is not provided. Kindly check and provide.	
AQ2	Table 2 and Fig. 5 were received; however, no citation were provided in the manuscript. Please check and confirm the inserted citation of Fig. 5 and Table 2 are correct. If not, please suggest an alternative citation. Please note that figures and tables should be cited in numerical order in the text and should be inside the main body of the text.	
AQ3	Table 5 citation has been changed to Table 4. Kindly check and confirm.	
AQ4	As References [12] and [43] are same, we have deleted the duplicate reference and renumbered accordingly. Please check and confirm.	